

## Determination of resistance against the transmission of charged particles of Rhenium-Boron (Re-B) based alloys

Murat AYGÜN<sup>1\*</sup>



<sup>1</sup>Bitlis Eren University Faculty of Science and Literature Department of Physics

(ORCID: [0000-0002-4276-3531](https://orcid.org/0000-0002-4276-3531))

**Keywords:** Stopping power, Abstract

Electron, Heavy charged particle  
SRIM, ESTAR.

In this study, the resistance of the Rhenium-Boron (Re-B) based alloys against the transmission of charged particles such as electrons, protons, alpha particles, carbon, and oxygen was investigated using the stopping power as the defining quantity. For this, the collision, radiative/nuclear, total stopping powers, and projected range of the charged particles in the Re40-B60, Re50-B50, Re58-B42, and Re60-B40 alloys were calculated using the ESTAR, and the Stopping and Range of Ions in Materials (SRIM) Monte Carlo code. It was found that the stopping powers of the heavy charged particles tended to decrease with increasing the rhenium concentration. These results suggest that the boron element is more suitable for heavy charged particle shielding materials compared to the rhenium element.

### 1. Introduction

Radiation is the emission or transfer of energy in the form of electromagnetic waves or particles and can be classified as ionizing and non-ionizing radiation. In this context, ionizing radiation can be evaluated in three categories: charged particles, photons and neutrons. Electrons (e), protons (p), alpha ( $\alpha$ ), and heavy ions ( $A>4$ ) are considered as charged particles. The importance of radiation protection is increasing because the use of radiation emitting devices is very common in fields such as nuclear reactors, medicine, agriculture, and so on [1]. Developing radiation shielding materials and their usage is one method to reduce the radiation exposure risk [2]. Therefore, explaining the interaction of charged particles and matter will be important for radiation protection and a better understanding of radiation with various materials.

It is significant to determine the radiation shielding attitude of a material against charged particles such as electrons, protons, and alpha rays, and elements such as carbon and oxygen. In this context, the stopping power of the charged particles passing through the material is an important shielding

parameter [3]. The stopping power is the rate of energy loss per unit path length in the target material [4], and has two cases, such as collisions and radiative/nuclear interactions. The total stopping power can be calculated as the sum of these two states.

Rhenium-based alloys are important materials evaluated in different fields of nuclear technology, such as nuclear fusion and atom probe tomography (APT) system components [5, 6]. For example,  $^{186}\text{Re}$  has been applied to clinical radiotherapy applications by Mastren et al. [7]. Klueh et al. [8] have shown that the radiation shielding properties of an example stainless steel have increased with the addition of the Re. Korkut et al. [6] have developed novel high-temperature-resistant materials with different concentrations of Re and B (Re40-B60, Re50-B50, Re58-B42, and Re60-B40) in order to determine the neutron-shielding performances. However, it has been seen that the stopping powers and ranges for charged particles have not been determined for these new and important materials when we have searched the literature. Therefore, we think that eliminating this deficiency will be important.

\* Corresponding author: [maygun@beu.edu.tr](mailto:maygun@beu.edu.tr)

Received: 20.10.2022, Accepted: 23.02.2023

In this study, we calculate collision, radiative/nuclear and total stopping powers for charged particles such as electron (e), proton (H), alpha (He), carbon (C) and oxygen (O) for Re40-B60, Re50-B50, Re58-B42 and Re60-B40 alloys by using ESTAR provided by the National Institute of Standards and Technology (NIST) [9] and Stopping and Range of Ions in Materials (SRIM)-2013 [10] programs. In addition, we calculate ranges for all alloys and compare all the results with each other.

## 2. Material and Method

### 2.1. Stopping Power and Projected Range

The stopping power is the resistance of a material against the charged particles [11]. The stopping power can be evaluated as the sum of electronic (collisional) stopping power and nuclear stopping power. The electronic stopping power states the energy losses due to electronic interactions, while the nuclear stopping power expresses the energy losses based on the elastic collisions between the ion and the nuclei of atoms in the material. The stopping power depends on the magnitude of the radiation mass, charge, and kinetic energy as well as the effective atomic number and atomic density of the interacting medium [11]. In this context, the stopping power formula for heavy charged particles can be written as [12]

$$-\frac{dE}{dx} = 4\pi r_0^2 z^2 \frac{m_0 c^2}{\beta^2} N Z \left[ \ln \left( \frac{2m_0 c^2}{I} \beta^2 \gamma^2 \right) - \beta^2 \right] \quad (1)$$

and the stopping power formula for electrons can be given by

$$-\frac{dE}{dx} = 4\pi r_0^2 \frac{m_0 c^2}{\beta^2} N Z \left\{ \ln \left( \frac{\beta \gamma \sqrt{\gamma-1}}{I} m_0 c^2 \right) + \frac{1}{2\gamma^2} \left[ \frac{(\gamma-1)^2}{8} + 1 - (\gamma^2 + 2\gamma - 1) \ln 2 \right] \right\} \quad (2)$$

where  $dE/dx$  is the charged particle stopping power,  $r_0$  is the classical electron radius,  $z$  is the charge of the incident particle,  $m_0 c^2$  is the rest energy of the electron,  $\beta$  is the relative phase velocity of the particle,  $N$  is the particle density in the material through which the charged particle travels,  $Z$  is the atomic number of the material and  $I$  is mean excitation energy. If a compound or mixture of

elements is concerned,  $\langle I \rangle$  must be calculated according to Bethe theory as follows

$$\langle I \rangle = \exp \left\{ \frac{\left[ \sum_j \left( \frac{Z_j}{A_j} \right) \ln I_j \right]}{\sum_j \left( \frac{w_j Z_j}{A_j} \right)} \right\} \quad (3)$$

where  $w_j$ ,  $Z_j$  and  $A_j$  are the weight fraction, atomic number, and atomic weight of the  $j$ th element, respectively [13]. In this study, the collision, nuclear, and total stopping power parameters of the charged particles for Re40-B60, Re50-B50, Re58-B42 and Re60-B40 alloys are calculated. In this respect, the weight compositions and densities of the alloys are given in Table 1.

**Table 1.** Weight compositions and densities of the alloys [6]

Sample name	Rhenium (%)	Boron (%)	$\rho$ (g/cm <sup>3</sup> )
Re40-B60	40	60	9.81
Re50-B50	50	50	11.68
Re58-B42	58	42	13.17
Re60-B40	60	40	13.55

The projected range ( $R_p$ ) is a significant parameter for determining nuclear radiation shielding and interactions with materials [14]. The  $R_p$  is assumed as the distance traveled by the particle within the medium previous to lose all of its energy [15]. The  $R_p$  of charged particles can be written as

$$R_p(E) = \int_0^E \frac{1}{\left( -\frac{dE}{dx} \right)} dE \quad (4)$$

where  $E$  is the charged particle energy (MeV) and  $x$  is distance of the charged particles travel through a material (in m).

### 2.2. Computer Programs

The Bethe formula is generally a good approximation for high-energy charged particles (>0.5 MeV) [16,17], although it is not very valid for low-energy

charged particles. On the other hand, the Bethe formula based on Barkas-Andersen [18] and Bloch [19] corrections can be more suitable for the low-energy regime [17].

The SRIM is a computer code containing the stopping and range ions in matter [10]. It can calculate electronic and nuclear stopping powers according to the ion type, its energy, and the target material type. Also, it uses the Köln Core and Bond (CAB) approach to estimate the stopping power in compounds [16]. There are versions such as SRIM-1998, SRIM-2003, SRIM-2006, SRIM-2008, and SRIM-2013 in the literature. In this work, the SRIM-2013 code, which is the latest version, is used to calculate the stopping power values and projected range versus particle energy.

The ESTAR is a computer code that can calculate collision, radiative, total stopping powers, and range of electrons for any element, compound, or mixture at any set of kinetic energies between 1 keV and 10 GeV. The ESTAR code needs to be entered the information such as the atomic composition, density, and excitation energy of the material. In the program, firstly, the analyzed material is determined, and then the desired or default energies are entered [9].

## Results and Discussion

The total stopping power for electron interaction can be divided into two parts: collisional stopping power and radiative stopping power. The collision, radiative, and total stopping powers of the electrons for the Re40-B60, Re50-B50, Re58-B42, and Re60-B40 alloys at energies between 0.1 and 1000 MeV were calculated, and shown the variation with energy in Fig. 1. Additionally, to make a comparison, the collision, radiative, and total stopping powers for energies up to 15 MeV were given in Table 2. The total stopping powers of the electrons are among 1.334-71.40 MeV cm<sup>2</sup>/g for Re40-B60, 1.298-84.21 MeV cm<sup>2</sup>/g for Re50-B50, 1.269-94.47 MeV cm<sup>2</sup>/g for Re58-B42 and 1.262-97.03 MeV cm<sup>2</sup>/g for Re60-B40. For the electron, the total stopping powers generally decrease to the maximum of kinetic energy at 1.00 MeV, and then increase gradually as the energy increases. It was observed that the stopping powers of electrons decreased with the increase of the Re element and the decrease of the B element. As a result, we can say that the stopping powers of electrons for the B element are higher than those for the Re element.

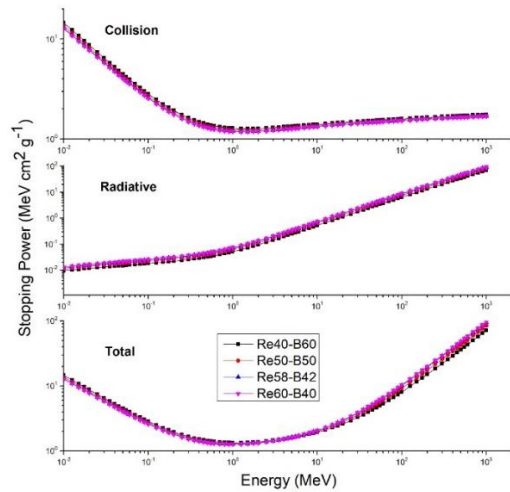


**Figure 1.** Variations of collision, radiative and total stopping powers of electron as a function of kinetic energy for Re40-B60, Re50-B50, Re58-B42, and Re60-B40 alloys

The collision, nuclear, and total stopping powers of the proton calculated for the alloys were given in Table 3, and were also displayed the variation with energy in Fig. 2. For the proton, it was seen that the total stopping powers decrease with increasing kinetic energy and have a maximum value at a kinetic energy of 0.1 MeV. The highest values of the total stopping powers of protons are at 0.1 MeV with value of 153.772 MeV cm<sup>2</sup>/g, 138.356 MeV cm<sup>2</sup>/g, 129.447 MeV cm<sup>2</sup>/g and 127.545 MeV cm<sup>2</sup>/g for Re40-B60, Re50-B50, Re58-B42 and Re60-B40, respectively. The smallest values of the total stopping powers of protons are at 1000 MeV, with values of 1.261 MeV cm<sup>2</sup>/g, 1.246 MeV cm<sup>2</sup>/g, 1.238 MeV cm<sup>2</sup>/g and 1.236 MeV cm<sup>2</sup>/g for Re40-B60, Re50-B50, Re58-B42 and Re60-B40, respectively. Also, the highest stopping power value (153.772 MeV cm<sup>2</sup> g<sup>-1</sup>) was found for the Re40-B60 alloy, and the smallest stopping power value (1.236 MeV cm<sup>2</sup> g<sup>-1</sup>) for the proton particle was recorded for the Re60-B40 alloy. Afterward, proton particle total stopping power for all the alloys are reduced progressively with increasing kinetic energy. It was realized that the total proton stopping powers decreased with the increase of the rhenium element and the decrease of the boron element. Thus, we can say that the proton stopping power of the B element is higher than the Re element.

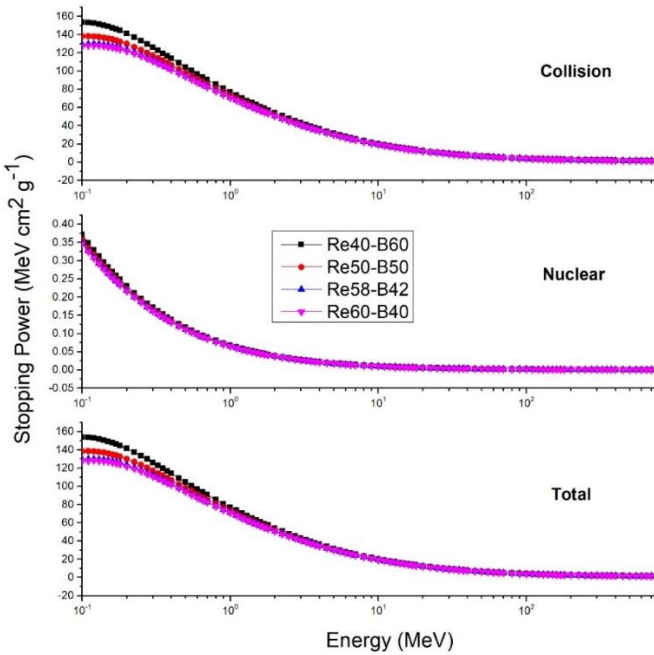


**Figure 2.** Variations of collision, nuclear and total stopping powers of proton as a function of kinetic energy for Re40-B60, Re50-B50, Re58-B42, and Re60-B40 alloys

The collision, nuclear, and total stopping powers of the alpha particles calculated for the alloys were listed in Table 4 and were presented the variation with energy in Fig. 3. For the alpha particles, it was found that the total stopping powers increase with increasing kinetic energy and have a maximum value at the kinetic energies of 0.9-1.0 MeV. The total stopping power parameters of alpha are among 8.611-478.782 MeV cm<sup>2</sup>/g for Re40-B60, 8.492-438.653 MeV cm<sup>2</sup>/g for Re50-B50, 8.423-416.365 MeV cm<sup>2</sup>/g for Re58-B42 and 8.409-411.662 MeV cm<sup>2</sup>/g for Re60-B40. It was observed that the total alpha stopping powers decreased with the increase of the Re element and the decrease of the B element. As a result, we can state that the alpha stopping power of the B element is higher than the Re element.

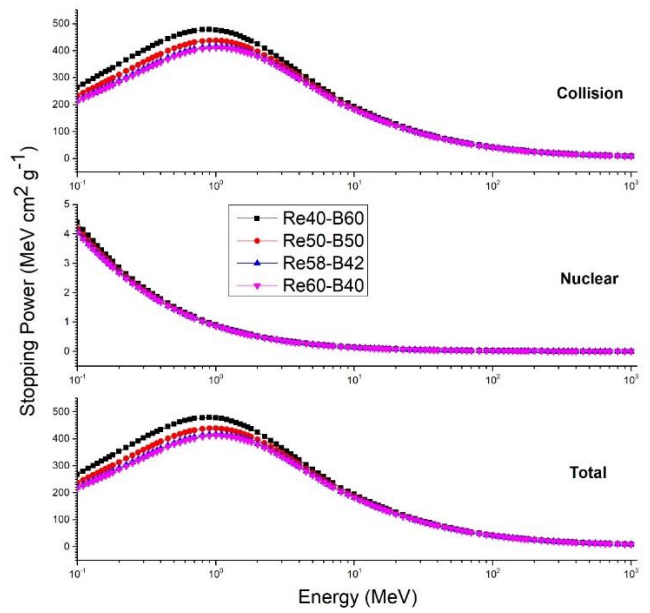


**Figure 3.** Variations of collision, nuclear and total stopping powers of alpha as a function of kinetic energy for Re40-B60, Re50-B50, Re58-B42, and Re60-B40 alloys

The collision, nuclear and total stopping powers of the carbon for the alloys were calculated and given in Table 5, and were also shown the variation with energy in Fig. 4. For the carbon ions, it was found that the total stopping powers increase when the kinetic energy increases. The highest values of the total stopping powers of carbon ions are at 6.5 MeV with a value of 2245.294 MeV cm<sup>2</sup>/g, at 7.0 MeV with a value of 2124.955 MeV cm<sup>2</sup>/g, at 7.0 MeV with a value of 2055.901 MeV cm<sup>2</sup>/g and at 7.0 MeV with a value of 2040.889 MeV cm<sup>2</sup>/g for Re40-B60, Re50-B50, Re58-B42 and Re60-B40, respectively. The smallest values of the total stopping powers of carbon are at 1000 MeV with values of 155.257 MeV cm<sup>2</sup>/g, 152.756 MeV cm<sup>2</sup>/g, 151.355 MeV cm<sup>2</sup>/g and 151.055 MeV cm<sup>2</sup>/g for Re40-B60, Re50-B50, Re58-B42 and Re60-B40, respectively. It was noticed that the total carbon stopping powers decreased with the increase of the Re element and the decrease of the B element. Hence, we can remark that the carbon stopping power of the B element is higher than the Re element.

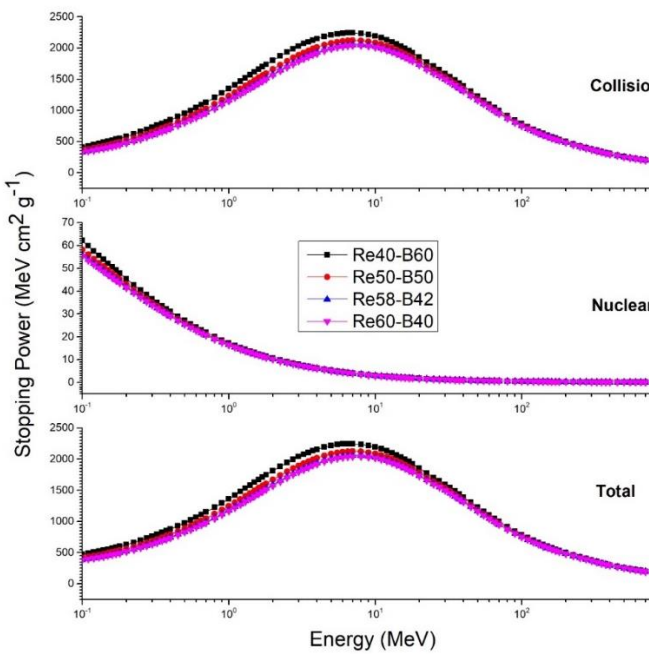


**Figure 4.** Variations of collision, nuclear and total stopping powers of carbon as a function of kinetic energy for Re40-B60, Re50-B50, Re58-B42, and Re60-B40 alloys

The collision, nuclear, and total stopping powers of the oxygen calculated for the alloys were given in Table 6 and were displayed the variation with energy in Fig. 5. For the oxygen ions, it was found that the total stopping powers increase with increasing kinetic energy and have a maximum value at kinetic energies of 10.0-11.0 MeV. The highest values of the total stopping powers of oxygen are at 10.0 MeV with a value of  $3239.727 \text{ MeV cm}^2/\text{g}$ , at 11.0 MeV with a value of  $3074.097 \text{ MeV cm}^2/\text{g}$ , at 11.0 MeV with a value of  $2979.019 \text{ MeV cm}^2/\text{g}$  and at 11.0 MeV with a value of  $2959.003 \text{ MeV cm}^2/\text{g}$  for Re40-B60, Re50-B50, Re58-B42 and Re60-B40, respectively. The smallest values of the total stopping powers of protons are at 1000 MeV with values of  $345.530 \text{ MeV cm}^2/\text{g}$ ,  $339.728 \text{ MeV cm}^2/\text{g}$ ,  $336.427 \text{ MeV cm}^2/\text{g}$  and  $335.726 \text{ MeV cm}^2/\text{g}$  for Re40-B60, Re50-B50, Re58-B42 and Re60-B40, respectively. It was observed that the total oxygen stopping power decreased with the increase of the Re element and the decrease of the B element. As a result, we can say that the oxygen stopping power of the B element is higher than the Re element.

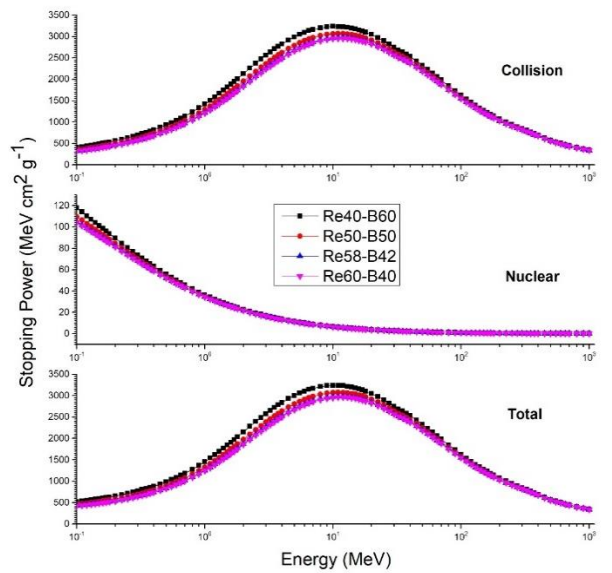


**Figure 5.** Variations of collision, nuclear and total stopping powers of oxygen as a function of kinetic energy for Re40-B60, Re50-B50, Re58-B42, and Re60-B40 alloys

Figure 6 shows the results of the projected range ( $R_p$ ) of charged particles for Re40-B60, Re50-B50, Re58-B42, and Re60-B40 alloys. Obviously, the projected range value increases with the increase of the kinetic energy of the incident charged particles. Proton particles can move deeper than alpha, carbon, and oxygen particles because they have less mass than alpha, carbon, and oxygen particles. The charged particle ranges decrease with an increasing concentration of the Re element. Thus, the range of heavy charged particles changes in order of Re40-B60 > Re50-B50 > Re58-B42 > Re60-B40.

**Table 2.** Collision, radiative and total stopping powers (MeV cm<sup>2</sup> g<sup>-1</sup>) for electrons

Energy (MeV)	Re40–B60			Re50–B50			Re58–B42			Re60–B40		
	$\left(\frac{dE}{dx}\right)_{Col.}$	$\left(\frac{dE}{dx}\right)_{Rad.}$	$\left(\frac{dE}{dx}\right)_{Total}$									
0.100	2.829	0.018	2.847	2.696	0.022	2.718	2.591	0.025	2.616	2.565	0.025	2.591
0.125	2.474	0.019	2.494	2.361	0.023	2.384	2.271	0.026	2.298	2.248	0.027	2.276
0.150	2.234	0.020	2.254	2.133	0.024	2.158	2.053	0.028	2.082	2.034	0.029	2.063
0.175	2.061	0.021	2.082	1.969	0.025	1.995	1.897	0.029	1.926	1.879	0.030	1.909
0.200	1.931	0.022	1.953	1.846	0.027	1.873	1.779	0.030	1.810	1.762	0.031	1.794
0.250	1.749	0.023	1.773	1.674	0.029	1.703	1.614	0.033	1.647	1.599	0.034	1.634
0.300	1.629	0.025	1.655	1.560	0.031	1.592	1.506	0.035	1.542	1.493	0.036	1.529
0.350	1.546	0.027	1.573	1.482	0.033	1.515	1.431	0.038	1.469	1.418	0.039	1.457
0.400	1.485	0.029	1.514	1.424	0.035	1.460	1.376	0.040	1.417	1.364	0.041	1.406
0.450	1.440	0.030	1.471	1.381	0.037	1.419	1.335	0.042	1.378	1.324	0.044	1.368
0.500	1.405	0.032	1.438	1.349	0.039	1.388	1.304	0.045	1.350	1.293	0.046	1.340
0.550	1.378	0.034	1.412	1.323	0.041	1.365	1.280	0.047	1.328	1.269	0.049	1.319
0.600	1.356	0.036	1.392	1.303	0.044	1.347	1.261	0.050	1.311	1.250	0.051	1.302
0.700	1.325	0.040	1.365	1.274	0.048	1.322	1.234	0.055	1.289	1.224	0.057	1.281
0.800	1.305	0.044	1.349	1.255	0.053	1.308	1.216	0.060	1.277	1.206	0.062	1.269
0.900	1.291	0.048	1.339	1.243	0.058	1.301	1.205	0.066	1.271	1.195	0.068	1.264
1.000	1.282	0.052	1.334	1.235	0.063	1.298	1.197	0.071	1.269	1.188	0.074	1.262
1.250	1.272	0.062	1.334	1.226	0.075	1.302	1.190	0.086	1.276	1.181	0.088	1.270

1.500	1.270	0.073	1.344	1.226	0.088	1.314	1.191	0.101	1.292	1.182	0.104	1.286
1.750	1.273	0.084	1.358	1.229	0.102	1.332	1.195	0.116	1.311	1.187	0.119	1.306
2.000	1.278	0.096	1.375	1.235	0.116	1.351	1.201	0.132	1.333	1.193	0.135	1.329
2.500	1.290	0.120	1.411	1.248	0.144	1.393	1.215	0.164	1.379	1.207	0.169	1.376
3.000	1.303	0.145	1.448	1.261	0.174	1.435	1.228	0.197	1.426	1.220	0.203	1.424
3.500	1.315	0.170	1.485	1.273	0.204	1.478	1.241	0.231	1.473	1.233	0.238	1.472
4.000	1.326	0.196	1.522	1.285	0.235	1.520	1.253	0.266	1.519	1.245	0.274	1.519
4.500	1.336	0.222	1.558	1.295	0.266	1.561	1.264	0.301	1.565	1.256	0.310	1.566
5.000	1.345	0.248	1.594	1.305	0.298	1.603	1.274	0.337	1.611	1.266	0.347	1.613
5.500	1.354	0.275	1.629	1.313	0.330	1.644	1.283	0.373	1.656	1.275	0.384	1.659
6.000	1.361	0.303	1.664	1.321	0.362	1.684	1.291	0.410	1.701	1.283	0.422	1.705
7.000	1.375	0.358	1.734	1.336	0.428	1.764	1.305	0.484	1.790	1.298	0.498	1.797
8.000	1.387	0.415	1.802	1.348	0.495	1.844	1.318	0.560	1.879	1.311	0.576	1.887
9.000	1.398	0.472	1.870	1.359	0.563	1.923	1.329	0.637	1.967	1.322	0.655	1.978
10.00	1.407	0.530	1.937	1.369	0.632	2.001	1.339	0.714	2.054	1.332	0.735	2.068
12.50	1.427	0.677	2.105	1.389	0.808	2.197	1.361	0.912	2.273	1.354	0.938	2.292
15.00	1.443	0.828	2.271	1.406	0.986	2.392	1.377	1.114	2.491	1.371	1.145	2.516

**Table 3.** Collision, nuclear and total stopping powers (MeV cm<sup>2</sup> g<sup>-1</sup>) for proton

Energy (MeV)	Re40–B60			Re50–B50			Re58–B42			Re60–B40		
	$\left(\frac{dE}{dx}\right)_{Col.}$	$\left(\frac{dE}{dx}\right)_{Nuc.}$	$\left(\frac{dE}{dx}\right)_{Total}$									
0.1	153.4	0.371	153.771	138.0	0.356	138.356	129.1	0.347	129.447	127.2	0.345	127.545
0.2	141.1	0.230	141.330	129.7	0.222	129.922	123.1	0.217	123.317	121.7	0.216	121.916
0.3	125.9	0.171	126.071	117.0	0.165	117.165	111.9	0.162	112.062	110.8	0.161	110.961
0.4	113.8	0.138	113.938	106.5	0.133	106.633	102.2	0.131	102.331	101.3	0.130	101.430
0.5	104.3	0.116	104.416	98.01	0.112	98.122	94.38	0.110	94.490	93.61	0.110	93.720
0.6	96.69	0.101	96.791	91.16	0.098	91.258	87.98	0.096	88.076	87.31	0.096	87.406
0.7	90.44	0.089	90.529	85.51	0.087	85.597	82.68	0.085	82.765	82.07	0.085	82.155
0.8	85.21	0.080	85.290	80.76	0.078	80.838	78.20	0.077	78.277	77.65	0.076	77.726
0.9	80.76	0.073	80.833	76.69	0.071	76.761	74.35	0.070	74.420	73.86	0.069	73.929
1.00	76.92	0.067	76.987	73.17	0.065	73.235	71.02	0.064	71.084	70.56	0.064	70.624
1.10	73.57	0.062	73.632	70.08	0.060	70.140	68.07	0.059	68.129	67.64	0.059	67.699
1.20	70.25	0.058	70.308	67.00	0.056	67.056	65.13	0.055	65.185	64.73	0.055	64.785
1.30	67.49	0.054	67.544	64.44	0.053	64.493	62.69	0.052	62.742	62.31	0.052	62.362
1.40	65.04	0.051	65.091	62.16	0.050	62.210	60.51	0.049	60.559	60.16	0.049	60.209
1.50	62.81	0.048	62.858	60.09	0.047	60.137	58.52	0.046	58.566	58.19	0.046	58.236
1.60	60.77	0.046	60.816	58.18	0.044	58.224	56.70	0.044	56.744	56.38	0.044	56.424
1.70	58.89	0.043	58.933	56.43	0.042	56.472	55.01	0.042	55.052	54.71	0.041	54.751
1.80	57.15	0.041	57.191	54.80	0.040	54.840	53.45	0.040	53.490	53.16	0.040	53.200

2.00	54.02	0.038	54.058	51.87	0.037	51.907	50.63	0.036	50.666	50.37	0.036	50.406
2.25	50.66	0.034	50.694	48.71	0.033	48.743	47.58	0.033	47.613	47.35	0.033	47.383
2.50	47.77	0.031	47.801	45.98	0.031	46.011	44.96	0.030	44.990	44.74	0.030	44.770
2.75	45.25	0.029	45.279	43.60	0.028	43.628	42.66	0.028	42.688	42.46	0.028	42.488
3.00	43.03	0.027	43.057	41.51	0.026	41.536	40.63	0.026	40.656	40.44	0.026	40.466
3.25	41.06	0.025	41.085	39.64	0.025	39.665	38.82	0.024	38.844	38.65	0.024	38.674
3.50	39.29	0.024	39.314	37.96	0.023	37.983	37.20	0.023	37.223	37.03	0.023	37.053
3.75	37.69	0.022	37.712	36.45	0.022	36.472	35.73	0.021	35.751	35.57	0.021	35.591
4.00	36.25	0.021	36.271	35.07	0.021	35.091	34.39	0.020	34.410	34.25	0.020	34.270
4.50	33.71	0.019	33.729	32.66	0.019	32.679	32.05	0.018	32.068	31.92	0.018	31.938
5.00	31.57	0.017	31.587	30.61	0.017	30.627	30.05	0.017	30.067	29.94	0.017	29.957
6.00	28.11	0.015	28.125	27.30	0.014	27.314	26.83	0.014	26.844	26.73	0.014	26.744
7.00	25.43	0.013	25.443	24.73	0.013	24.743	24.33	0.012	24.342	24.24	0.012	24.252
8.00	23.29	0.011	23.301	22.67	0.011	22.681	22.31	0.011	22.321	22.24	0.011	22.251
9.00	21.52	0.010	21.530	20.97	0.010	20.980	20.65	0.010	20.660	20.58	0.010	20.590
10.00	20.04	0.009	20.049	19.54	0.009	19.549	19.25	0.009	19.259	19.19	0.009	19.199
11.00	18.78	0.009	18.789	18.32	0.008	18.328	18.06	0.008	18.068	18.01	0.008	18.018
12.00	17.69	0.008	17.698	17.27	0.008	17.278	17.03	0.008	17.038	16.98	0.008	16.988
13.00	16.74	0.007	16.747	16.35	0.007	16.357	16.12	0.007	16.127	16.08	0.007	16.087
14.00	15.90	0.007	15.907	15.53	0.007	15.537	15.32	0.007	15.327	15.28	0.007	15.287
15.00	15.15	0.006	15.156	14.81	0.006	14.816	14.61	0.006	14.616	14.57	0.006	14.576

**Table 4.** Collision, nuclear and total stopping powers (MeV cm<sup>2</sup> g<sup>-1</sup>) for alpha

Energy (MeV)	Re40–B60			Re50–B50			Re58–B42			Re60–B40		
	$\left(\frac{dE}{dx}\right)_{Col.}$	$\left(\frac{dE}{dx}\right)_{Nuc.}$	$\left(\frac{dE}{dx}\right)_{Total}$									
0.1	263.9	4.395	268.295	233.4	4.180	237.580	215.9	4.056	219.956	212.2	4.030	216.230
0.2	349.8	2.864	352.664	310.8	2.749	313.549	288.3	2.683	290.983	283.5	2.669	286.169
0.3	400.1	2.182	402.282	357.1	2.103	359.203	332.3	2.057	334.357	327.1	2.048	329.148
0.4	432.5	1.785	434.285	388.0	1.724	389.724	362.4	1.689	364.089	357.0	1.681	358.681
0.5	453.3	1.521	454.821	408.7	1.471	410.171	383.1	1.443	384.543	377.6	1.437	379.037
0.6	466.2	1.331	467.531	422.3	1.289	423.589	397.1	1.265	398.365	391.7	1.260	392.960
0.7	473.6	1.187	474.787	430.8	1.151	431.951	406.2	1.130	407.330	400.9	1.125	402.025
0.8	477.1	1.074	478.174	435.6	1.042	436.642	411.7	1.023	412.723	406.7	1.019	407.719
0.9	477.8	0.982	478.782	437.7	0.953	438.653	414.6	0.936	415.536	409.7	0.933	410.633
1.00	476.4	0.906	477.306	437.7	0.880	438.580	415.5	0.865	416.365	410.8	0.862	411.662
1.10	473.5	0.842	474.342	436.3	0.818	437.118	414.9	0.804	415.704	410.3	0.801	411.101
1.20	469.6	0.787	470.387	433.7	0.765	434.465	413.1	0.752	413.852	408.7	0.750	409.450
1.30	464.9	0.739	465.639	430.3	0.719	431.019	410.5	0.707	411.207	406.2	0.705	406.905
1.40	459.6	0.698	460.298	426.3	0.679	426.979	407.2	0.668	407.868	403.1	0.666	403.766
1.50	453.9	0.661	454.561	421.9	0.643	422.543	403.4	0.633	404.033	399.5	0.631	400.131
1.60	448.0	0.628	448.628	417.1	0.611	417.711	399.3	0.602	399.902	395.5	0.600	396.100
1.70	441.9	0.599	442.499	412.1	0.583	412.683	394.9	0.574	395.474	391.2	0.572	391.772
1.80	435.7	0.572	436.272	406.9	0.557	407.457	390.3	0.549	390.849	386.8	0.547	387.347

2.00	423.4	0.526	423.926	396.4	0.513	396.913	380.9	0.505	381.405	377.6	0.503	378.103
2.25	408.1	0.479	408.579	383.2	0.467	383.667	368.9	0.460	369.360	365.8	0.458	366.258
2.50	393.5	0.440	393.940	370.4	0.429	370.829	357.0	0.423	357.423	354.2	0.421	354.621
2.75	379.6	0.407	380.007	358.0	0.397	358.397	345.6	0.391	345.991	342.9	0.390	343.290
3.00	366.4	0.379	366.779	346.2	0.370	346.570	334.6	0.365	334.965	332.1	0.364	332.464
3.25	354.1	0.355	354.455	335.1	0.347	335.447	324.2	0.342	324.542	321.9	0.341	322.241
3.50	342.5	0.335	342.835	324.6	0.327	324.927	314.3	0.322	314.622	312.1	0.321	312.421
3.75	331.6	0.316	331.916	314.7	0.309	315.009	304.9	0.304	305.204	302.9	0.303	303.203
4.00	321.4	0.300	321.700	305.4	0.293	305.693	296.1	0.289	296.389	294.2	0.288	294.488
4.50	302.8	0.272	303.072	288.3	0.266	288.566	279.9	0.262	280.162	278.1	0.261	278.361
5.00	286.4	0.249	286.649	273.1	0.243	273.343	265.4	0.240	265.640	263.8	0.240	264.040
6.00	258.6	0.214	258.814	247.2	0.209	247.409	240.7	0.206	240.906	239.3	0.206	239.506
7.00	236.1	0.188	236.288	226.2	0.184	226.384	220.5	0.182	220.682	219.3	0.181	219.481
8.00	217.5	0.168	217.668	208.8	0.164	208.964	203.7	0.162	203.862	202.7	0.162	202.862
9.00	205.3	0.152	205.452	197.4	0.149	197.549	192.8	0.147	192.947	191.9	0.147	192.047
10.00	193.5	0.139	193.639	186.3	0.136	186.436	182.2	0.134	182.334	181.3	0.134	181.434
11.00	183.2	0.128	183.328	176.6	0.126	176.726	172.8	0.124	172.924	172.0	0.124	172.124
12.00	174.1	0.119	174.219	168.0	0.117	168.117	164.5	0.115	164.615	163.7	0.115	163.815
13.00	166.0	0.111	166.111	160.3	0.109	160.409	157.0	0.108	157.108	156.4	0.107	156.507
14.00	158.8	0.104	158.904	153.5	0.102	153.602	150.4	0.101	150.501	149.7	0.101	149.801
15.00	152.3	0.098	152.398	147.3	0.096	147.396	144.4	0.095	144.495	143.8	0.095	143.895

**Table 5.** Collision, nuclear and total stopping powers (MeV cm<sup>2</sup> g<sup>-1</sup>) for carbon

Energy (MeV)	Re40–B60			Re50–B50			Re58–B42			Re60–B40		
	$\left(\frac{dE}{dx}\right)_{Col.}$	$\left(\frac{dE}{dx}\right)_{Nuc.}$	$\left(\frac{dE}{dx}\right)_{Total}$									
0.1	410.9	62.16	473.060	359.9	58.10	418.000	330.5	55.77	386.270	324.3	55.28	379.580
0.2	583.1	45.40	628.500	517.9	43.09	560.990	480.4	41.75	522.150	472.4	41.47	513.870
0.3	725.1	36.63	761.730	650.9	34.99	685.890	608.1	34.05	642.150	599.1	33.85	632.950
0.4	845.5	31.06	876.560	763.6	29.79	793.390	716.5	29.05	745.550	706.5	28.90	735.400
0.5	949.9	27.15	977.050	861.2	26.10	887.300	810.1	25.50	835.600	799.2	25.37	824.570
0.6	1043	24.23	1067.230	948.0	23.34	971.340	893.2	22.82	916.020	881.6	22.71	904.310
0.7	1128	21.95	1149.950	1027	21.17	1048.170	968.8	20.72	989.520	956.4	20.63	977.030
0.8	1206	20.10	1226.100	1100	19.42	1119.420	1038	19.02	1057.020	1025	18.94	1043.940
0.9	1278	18.58	1296.580	1167	17.97	1184.970	1103	17.61	1120.610	1089	17.53	1106.530
1.00	1345	17.30	1362.300	1229	16.74	1245.740	1162	16.42	1178.420	1148	16.35	1164.350
1.10	1407	16.21	1423.210	1287	15.69	1302.690	1218	15.40	1233.400	1203	15.33	1218.330
1.20	1464	15.26	1479.260	1341	14.79	1355.790	1269	14.51	1283.510	1254	14.45	1268.450
1.30	1518	14.43	1532.430	1391	13.99	1404.990	1318	13.73	1331.730	1302	13.68	1315.680
1.40	1567	13.70	1580.700	1437	13.28	1450.280	1363	13.04	1376.040	1347	12.99	1359.990
1.50	1613	13.04	1626.040	1481	12.65	1493.650	1405	12.43	1417.430	1389	12.38	1401.380
1.60	1656	12.45	1668.450	1522	12.09	1534.090	1444	11.87	1455.870	1428	11.83	1439.830
1.70	1696	11.92	1707.920	1560	11.57	1571.570	1481	11.37	1492.370	1465	11.33	1476.330
1.80	1733	11.44	1744.440	1595	11.11	1606.110	1516	10.92	1526.920	1499	10.88	1509.880

2.00	1800	10.59	1810.590	1660	10.29	1670.290	1579	10.12	1589.120	1562	10.08	1572.080
2.25	1872	9.710	1881.710	1730	9.442	1739.442	1648	9.288	1657.288	1631	9.255	1640.255
2.50	1933	8.978	1941.978	1790	8.735	1798.735	1708	8.596	1716.596	1690	8.566	1698.566
2.75	1985	8.359	1993.359	1842	8.137	1850.137	1759	8.009	1767.009	1741	7.982	1748.982
3.00	2029	7.828	2036.828	1886	7.623	1893.623	1803	7.505	1810.505	1786	7.479	1793.479
3.25	2067	7.366	2074.366	1924	7.176	1931.176	1842	7.066	1849.066	1825	7.043	1832.043
3.50	2099	6.961	2105.961	1957	6.783	1963.783	1876	6.681	1882.681	1858	6.659	1864.659
3.75	2126	6.602	2132.602	1986	6.435	1992.435	1905	6.339	1911.339	1888	6.319	1894.319
4.00	2149	6.282	2155.282	2010	6.125	2016.125	1930	6.034	1936.034	1913	6.015	1919.015
4.50	2185	5.734	2190.734	2049	5.593	2054.593	1971	5.512	1976.512	1954	5.494	1959.494
5.00	2210	5.281	2215.281	2077	5.153	2082.153	2001	5.080	2006.080	1985	5.064	1990.064
6.00	2237	4.575	2241.575	2110	4.467	2114.467	2037	4.405	2041.405	2022	4.392	2026.392
7.00	2241	4.048	2245.048	2121	3.955	2124.955	2052	3.901	2055.901	2037	3.889	2040.889
8.00	2232	3.638	2235.638	2117	3.555	2120.555	2051	3.508	2054.508	2037	3.498	2040.498
9.00	2214	3.309	2217.309	2104	3.235	2107.235	2041	3.192	2044.192	2028	3.183	2031.183
10.00	2190	3.038	2193.038	2084	2.971	2086.971	2024	2.933	2026.933	2011	2.925	2013.925
11.00	2161	2.812	2163.812	2060	2.751	2062.751	2001	2.715	2003.715	1989	2.708	1991.708
12.00	2129	2.619	2131.619	2032	2.563	2034.563	1976	2.530	1978.530	1964	2.523	1966.523
13.00	2096	2.453	2098.453	2002	2.401	2004.401	1948	2.371	1950.371	1936	2.364	1938.364
14.00	2062	2.308	2064.308	1971	2.259	1973.259	1919	2.231	1921.231	1908	2.225	1910.225
15.00	2027	2.181	2029.181	1939	2.135	1941.135	1888	2.109	1890.109	1878	2.103	1880.103

**Table 6.** Collision, nuclear and total stopping powers (MeV cm<sup>2</sup> g<sup>-1</sup>) for oxygen

Energy (MeV)	Re40–B60			Re50–B50			Re58–B42			Re60–B40		
	$\left(\frac{dE}{dx}\right)_{Col.}$	$\left(\frac{dE}{dx}\right)_{Nuc.}$	$\left(\frac{dE}{dx}\right)_{Total}$									
0.1	401.2	117.9	519.100	350.8	109.6	460.4	321.8	104.9	426.700	315.7	103.9	419.600
0.2	565.3	89.48	654.780	498.4	84.62	583.02	459.9	81.83	541.730	451.8	81.24	533.040
0.3	697.9	73.68	771.580	621.8	70.20	692	578.0	68.19	646.190	568.7	67.77	636.470
0.4	818.9	63.31	882.210	735.0	60.57	795.57	686.8	59.00	745.800	676.6	58.67	735.270
0.5	931.6	55.86	987.460	840.4	53.61	894.01	787.9	52.31	840.210	776.7	52.03	828.730
0.6	1038	50.21	1088.210	939.4	48.28	987.68	882.7	47.17	929.870	870.6	46.94	917.540
0.7	1139	45.74	1184.740	1033	44.06	1077.06	972.6	43.09	1015.690	959.7	42.88	1002.580
0.8	1236	42.10	1278.100	1123	40.61	1163.61	1059	39.75	1098.750	1045	39.56	1084.560
0.9	1330	39.07	1369.070	1210	37.73	1247.73	1141	36.95	1177.950	1126	36.79	1162.790
1.00	1419	36.51	1455.510	1293	35.28	1328.28	1220	34.58	1254.580	1205	34.43	1239.430
1.10	1506	34.30	1540.300	1373	33.17	1406.17	1297	32.53	1329.530	1280	32.39	1312.390
1.20	1588	32.38	1620.380	1450	31.34	1481.34	1370	30.74	1400.740	1353	30.61	1383.610
1.30	1667	30.68	1697.680	1523	29.72	1552.72	1440	29.16	1469.160	1422	29.04	1451.040
1.40	1743	29.18	1772.180	1593	28.28	1621.28	1507	27.76	1534.760	1489	27.65	1516.650
1.50	1815	27.84	1842.840	1661	26.99	1687.99	1571	26.50	1597.500	1553	26.39	1579.390
1.60	1884	26.63	1910.630	1725	25.83	1750.83	1633	25.36	1658.360	1614	25.27	1639.270
1.70	1949	25.53	1974.530	1786	24.77	1810.77	1692	24.33	1716.330	1672	24.24	1696.240
1.80	2012	24.53	2036.530	1844	23.81	1867.81	1748	23.40	1771.400	1727	23.31	1750.310

2.00	2127	22.77	2149.770	1953	22.12	1975.12	1853	21.74	1874.740	1831	21.66	1852.660
2.25	2257	20.94	2277.940	2075	20.35	2095.35	1971	20.01	1991.010	1948	19.94	1967.940
2.50	2371	19.41	2390.410	2183	18.87	2201.87	2076	18.57	2094.570	2053	18.50	2071.500
2.75	2471	18.11	2489.110	2280	17.62	2297.62	2170	17.34	2187.340	2146	17.28	2163.280
3.00	2560	16.99	2576.990	2365	16.54	2381.54	2253	16.28	2269.280	2230	16.22	2246.220
3.25	2638	16.01	2654.010	2442	15.59	2457.59	2328	15.35	2343.350	2304	15.30	2319.300
3.50	2708	15.15	2723.150	2510	14.76	2524.76	2395	14.54	2409.540	2371	14.49	2385.490
3.75	2770	14.39	2784.390	2570	14.02	2584.02	2456	13.81	2469.810	2431	13.77	2444.770
4.00	2824	13.71	2837.710	2625	13.36	2638.36	2510	13.16	2523.160	2486	13.12	2499.120
4.50	2917	12.54	2929.540	2718	12.23	2730.23	2603	12.05	2615.050	2579	12.01	2591.010
5.00	2990	11.57	3001.570	2792	11.29	2803.29	2679	11.13	2690.130	2655	11.09	2666.090
6.00	3095	10.05	3105.050	2902	9.816	2911.816	2791	9.679	2800.679	2768	9.650	2777.650
7.00	3161	8.917	3169.917	2974	8.710	2982.71	2867	8.591	2875.591	2844	8.566	2852.566
8.00	3201	8.029	3209.029	3020	7.847	3027.847	2916	7.742	2923.742	2894	7.719	2901.719
9.00	3223	7.315	3230.315	3048	7.151	3055.151	2947	7.057	2954.057	2926	7.037	2933.037
10.00	3233	6.727	3239.727	3063	6.578	3069.578	2965	6.493	2971.493	2944	6.475	2950.475
11.00	3232	6.233	3238.233	3068	6.097	3074.097	2973	6.019	2979.019	2953	6.003	2959.003
12.00	3225	5.813	3230.813	3065	5.687	3070.687	2973	5.615	2978.615	2953	5.600	2958.600
13.00	3212	5.449	3217.449	3056	5.333	3061.333	2967	5.266	2972.266	2948	5.252	2953.252
14.00	3195	5.132	3200.132	3043	5.024	3048.024	2956	4.961	2960.961	2938	4.948	2942.948
15.00	3175	4.853	3179.853	3027	4.751	3031.751	2942	4.692	2946.692	2924	4.680	2928.680

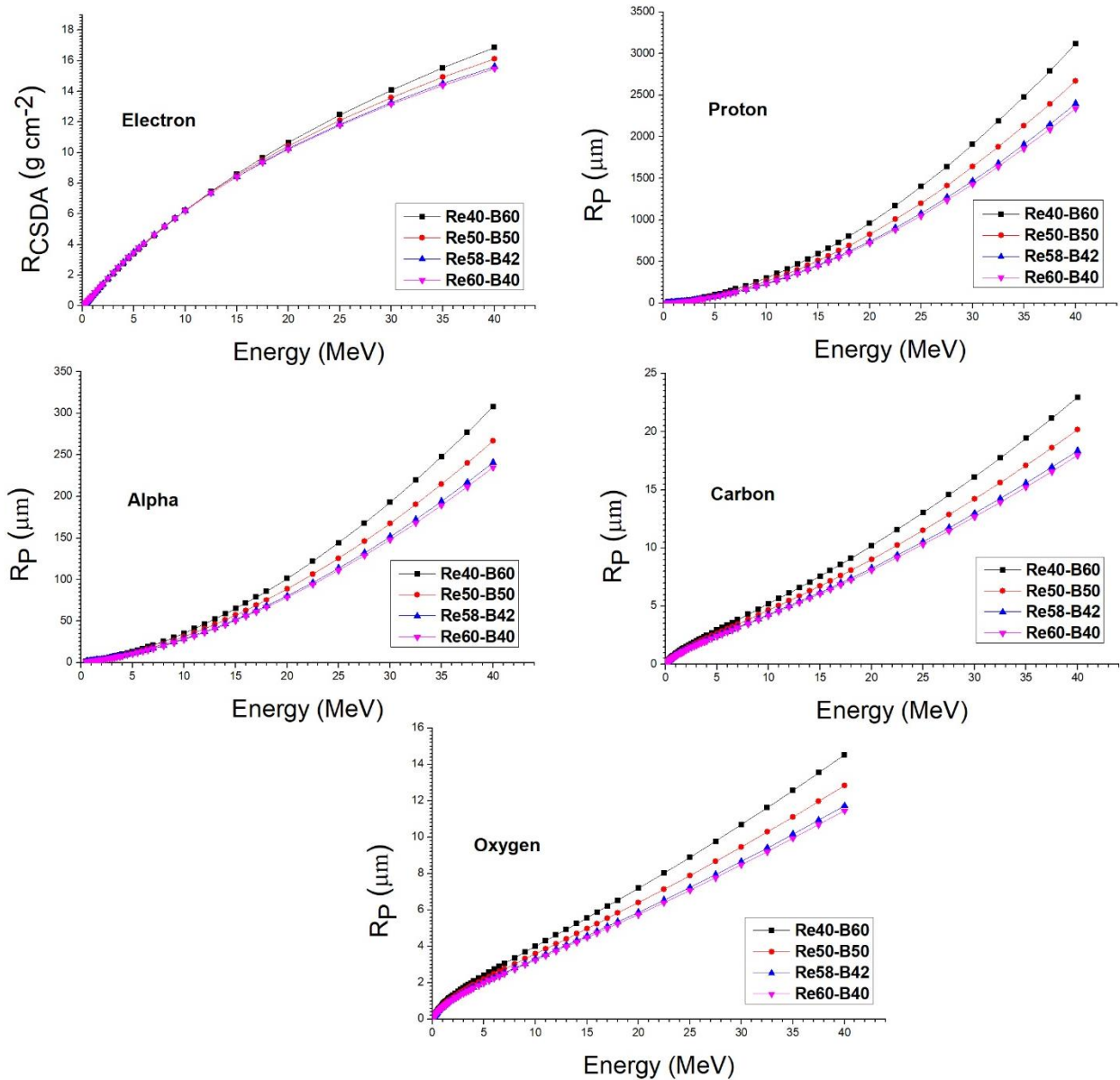


**Figure 6.** Variation of range ( $R$ ) as a function of kinetic energy in Re40-B60, Re50-B50, Re58-B42, and Re60-B40 alloys shown for electron, proton, alpha, carbon and oxygen.

#### 4. Conclusion and Suggestions

In the present research, we calculated collision, nuclear, and total stopping powers for charged particles such as electron, proton, alpha, carbon, and oxygen for Re60-B40, Re58-B42, Re50-B50, and Re40-B60 alloys by using the ESTAR and SRIM-2013 programs. We compared all the results with each other. The total stopping powers of charged particles (protons, alpha particles, heavy carbon, and oxygen ions) are minimum for the Re60-B40 alloy and maximum for the Re40-B60 alloy. Additionally, we noticed that the total stopping power decreased with the increase of the Re element and the decrease of the B element. Hence, we can deduce that the heavily charged particles have stopping powers in the following order: Re40-B60 > Re50-B50 > Re58-B42 > Re60-B40. Also, we can say that the charged particle ranges decrease with an increasing concentration of the Re element, and change in the order of Re40-B60 > Re50-B50 > Re58-B42 > Re60-B40.

#### Statement of Research and Publication Ethics

The study is complied with research and publication ethics

#### References

- [1] Z. Aygun, N. Yarbasi and M. Aygun, “Spectroscopic and radiation shielding features of Nemrut, Pasinler, Sarıkamış and İkizdere obsidians in Turkey: Experimental and theoretical study,” *Ceramics International*, vol. 47, pp. 34207-34217, 2021.
- [2] Z. Aygun and M. Aygun, “A theoretical evaluation on radiation shielding features of Van-Ercis and Rize-İkizdere (Türkiye) obsidians by using Phy-X/PSD code,” *Sigma Journal of Engineering and Natural Sciences*, vol. 40, pp. 845–854, 2022.
- [3] H. Osman and H. Gümüş, “Stopping power and CSDA range calculations of electrons and positrons over the 20 eV–1 GeV energy range in some water equivalent polymer gel dosimeters,” *Applied Radiation and Isotopes*, vol. 179, pp. 110024, 2022.
- [4] H. H. Andersen and P. Sigmund, “Stopping of heavy ions: a topical issue,” *Nuclear Instruments and Methods in Physics Research Section B: Beam Interactions with Materials and Atoms*, vol. 195, pp. 1-2, 2002.
- [5] A. Xu, D. E. J. Armstrong, C. Beck, M. P. Moody, G. D. W. Smith, P. A. J. Bagot and S. G. Roberts, “Ion irradiation induced clustering in W-Re-Ta, W-Re and W-Ta alloys: an atom probe tomography and nano indentation study,” *Acta Materialia*, vol. 124, pp. 71-78, 2017.
- [6] T. Korkut, H. Korkut, B. Aygün, Ö. Bayram, and A. Karabulut, “Investigation of high-temperature-resistant rhenium–boron neutron shields by experimental studies and Monte Carlo simulations,” *Nuclear Science and Techniques*, Vol. 29:102, pp. 2-5, 2018.
- [7] T. Mastren, V. Radchenko, H. T. Bach, E. R. Balkin, E. R. Birnbaum, M. Brugh, J. W. Engle, M. D. Gott, J. Guthrie, H. M. Hennkens, K. D. John, A. R. Ketring, M. Kuchuk, J. R. Maassen, C. M. Naranjo, F. M.

- Nortier, T. E. Phelps, S. S. Jurisson, D. S. Wilbur and M. E. Fassbender, "Bulk production and evaluation of high specific activity  $^{186}\text{Re}$  for cancer therapy using enriched  $^{186}\text{WO}_3$  targets in a proton beam," *Nuclear Medicine and Biology*, vol. 49, pp. 24-29, 2017.
- [8] R. L. Klueh, D. J. Alexander and M. A. Sokolov, "Effect of rhenium and osmium on mechanical properties of a 9Cr-2W-0.25V-0.07Ta-0.1C steel," *Journal of Nuclear Materials*, vol. 279, pp. 91–99, 2000.
  - [9] National Institute of Standards and Technology. [Online]. Available: <https://physics.nist.gov/PhysRefData/Star/Text/ESTAR.html> [Accessed: Oct. 17, 2022].
  - [10] J. F. Ziegler, "SRIM-the stopping and range of ions in matter," [Online]. Available: <http://www.srim.org> (2009) [Accessed: Oct. 17, 2022].
  - [11] J. S. Alzahrani, A. V. Lebedev, S. A. Avanesov, A. Hammoud, Z. A. Alrowaili, Z. M. M. Mahmoud, I. O. Olarinoye, C. Sriwunkum and M. S. Al-Buraihi, Synthesis, "Optical properties and radiation shielding performance of  $\text{TeO}_2\text{-Na}_2\text{O}\text{-BaO}\text{-WO}_3$  glass system," *Optik*, vol. 261, pp. 1-14, 2022.
  - [12] M. F. L'Annunziata, "Nuclear radiation, its interaction with matter and radioisotope decay," *Handbook of Radioactivity Analysis*, 1-122, 2003.
  - [13] S. M. Seltzer and M. J. Berger, "Evaluation of the collision stopping power of elements and compounds for electrons and positrons," *The International Journal of Applied Radiation and Isotopes*, vol. 33, pp. 1189–1218, 1982.
  - [14] W. Chaiphaksa, S. Yonphan, N. Chanthima, J. Kaewkhao and N. W. Sanwaranatee, "Computational approach of alpha and proton interaction of gadolinium bismuth borate glass system using SRIM programi," *Materials Today: Proceedings*, vol. 65, pp. 2416-2420, 2022.
  - [15] O. I. Sallam, A. M. Madbouly, N. L. Moussa and A. Abdel-Galil, "Impact of radiation on CoO-doped borate glass: lead-free radiation shielding," *Applied Physics A*, vol. 128, pp. 1-16, 2022.
  - [16] International Atomic Energy Agency (Nuclear Data Services), "Electronic stopping power of matter for ions.". [Online]. Available: <https://www-nds.iaea.org/stopping/> [Accessed: Oct. 17, 2022].
  - [17] S. R. Díaz, "Stopping power spectra of  $^4\text{He}$  ions in Zn, Cd and Pb-based semiconductors: A theoretical study for Rutherford Backscattering Spectroscopy analysis of metal chalcogenide thin films thickness," *Solid State Communications*, vol. 341, pp. 114580, 2022.
  - [18] P. Sigmund and A. Schinner, "Notes on barkas-andersen effect," *The European Physical Journal D*, vol. 68, pp. 318-325, 2014.
  - [19] L. E. Porter, "The barkas-effect correction to bethe–bloch stopping power," *Advances in Quantum Chemistry*, vol. 46, pp. 91-119, 2004.